

Miniaturized MIMO Antenna with Complementary Split Ring Resonators Loaded Superstrate for X-band Application

Karthigaiveni S (✉ dr.kk27@gmail.com)

NIT-Trichy: National Institute of Technology Tiruchirappalli

R Pandeewari

National Institute of Technology Tiruchirappalli

Deivalakshmi S

National Institute of Technology Tiruchirappalli

Research Article

Keywords: metamaterial, split ring resonator, MIMO, aperture coupling, isolation

Posted Date: March 10th, 2021

DOI: <https://doi.org/10.21203/rs.3.rs-290479/v1>

License:  This work is licensed under a Creative Commons Attribution 4.0 International License. [Read Full License](#)

Abstract

An aperture coupled two element metamaterial (MTM) antenna suitable for multiple input multiple output (MIMO) applications in the frequency band of 7.525-9.1GHz is proposed. This three-layered structure utilizes a vertical array of rectangular complementary split ring resonators (CSRR) between the contiguously placed circular non-bianisotropic complementary split ring resonator (NBCSRR) radiating elements for enhancement of isolation. This antenna achieves a maximum of 47dB isolation through this MNG structure insertion in the frequency band for $0.11 \lambda_0$ separation of the two antenna elements. The proposed antenna achieves a fractional -10dB impedance bandwidth of 18.94% and has a peak gain of 8.15dB. The efficiency of the antenna is 84.14% and the envelope correlation coefficient is less than 0.03 in the operating band. The antenna is low profile with an overall size of $0.85 \lambda_0 \times 0.45 \lambda_0 \times 0.133 \lambda_0$ and is suitable for X-band military applications.

1 | Introduction

MIMO antenna systems happen to be the vital cog of wireless communication system. The implementation of which currently has generated a plethora of issues to be sorted out by the researchers worldwide. One of the major issues in the development of multiple element antenna arrays for MIMO applications is mitigation of mutual coupling between the antenna elements that leads to severe degradation of system performance. This deleterious effect impacts antenna system parameters like bandwidth, gain, efficiency and impedance matching over the desired frequency range besides the radiation pattern and signal-to-interference-noise ratio (SINR). Since its vicious tentacles are spread over these crucial parameters, mutual coupling is the root cause of MIMO system performance degradation.

In multielement antennas, isolation enhancement is a major research problem that set off an extensive exploration of a variety of decoupling techniques. In the unsophisticated primitive techniques, miniaturization was the main casualty and the antenna systems became bulky and were not cost effective. Moreover, design complexity was an issue. MTM based antenna array systems are most suited for compact massive MIMO applications, since the compromise needed in the low-profile aspect of their design is almost negligible. While these exotic factitious materials revolutionized the realm of antenna design, isolation enhancement in MTM inspired multielement antennas useful in long term evolution (LTE) systems and array antennas for massive MIMO systems is a challenge currently confronting academicians and industrial scientists alike.

Mutual coupling in microstrip based and/or printed MTM antenna systems originates from surface wave propagation. Several novel decoupling techniques have been employed in MTM inspired antenna systems in the later years of current decade. Many innovative designs of multielement MTM antenna systems incorporating metasurface walls, electromagnetic bandgap (EBG) structures etc for decoupling the antenna elements have appeared in literature^{2,3}. Since mutual coupling suppression down to the levels of -30dB is desirable which is a thumb rule in MIMO antenna system designs, scientists worldwide started their journey in quest of directions for optimizing MIMO communication systems through enhanced isolation of array elements which constitute the array antenna. Measurements on prototypes of designs achieving mutual coupling suppression even down to less than -46.5dB levels have been reported in the literature⁴. The impact of MTM on antenna system designs is phenomenal⁵⁻⁸. Likewise, it offers many avenues to address a specific issue while designing an efficient multielement antenna system.

A class of MTM structures known as Electromagnetic bandgap structures or metasurface corrugations exhibit stop band and pass band characteristics for surface wave propagation. This property of EBG structures has been successfully utilized for attenuation of surface waves. Isolation and bandwidth enhancement have been achieved through two layer tunable EBG structures in unison with slit patch arrays placed between two monopole antennas^{3,9}. Two closely spaced meander line antennas are effectively decoupled through an MTM substrate and this antenna system is reported to achieve an isolation of 12-19dB over 5.1-5.9GHz frequency band². This simple design offers improved impedance matching and gain. Unwanted

frequency bands are notched for reducing multipath fading effects in four element UWB MIMO antenna system¹⁷ and envelope correlation coefficient (ECC) of less than 0.02 is maintained across the operating frequency band¹⁸.

An MTM mushroom wall has been used to improve isolation in a four element MIMO antenna system¹⁰. In this design, a crossed double layer mushroom wall structure integrated with substrate-integrated cavity-backed slot antenna elements and this system was shown to achieve an isolation of 42dB with an envelope correlation coefficient well below 0.02 within the operational band of 2.39-2.45GHz. In this design the height of the antenna system is rather high, limiting its use in MIMO applications. An array antenna decoupling surface (ADS) consisting of a thin substrate with flowery patterns of metal patches was tried out to suppress mutual coupling in a 4-element antenna and was found to bring down the mutual coupling to -30dB level¹¹. Here the unwanted coupled waves are cancelled by controlling the partially diffracted waves from the ADS through carefully designing the metallic patch patterns. Though this method is promising, its usefulness is limited and it can be applied only for 2 x 2 arrays. As the number of elements in an array antenna increases, the patch patterns on the ADS become very complicated¹.

A Jerusalem Cross (JC) MTM unit cells based thin planar lens MIMO antenna system with seven elements was constructed and demonstrated to achieve mutual coupling levels lower than -30dB which satisfies the threshold level desired by MIMO system requirement. However, compactness of the system suffers due to the large distance between the metalens and the element feeds and it is an issue that needs to be optimized for its suitability in MIMO communication systems¹². Mutual coupling reduction in Dielectric Resonator antennas useful for 60GHz MIMO system has been attained through a metasurface shield⁴. The constructed prototype achieved mutual coupling levels of -30 to -46.5dB in the 59.3–64.8GHz frequency band.

A MIMO antenna system employing a frequency selective surface (FSS) wall has been reported to achieve -30dB isolation levels¹³. The FSS walls of this system were optimized for the operating band of 57-63GHz to achieve this level which is a thumb-rule requirement in a MIMO system¹. Envelope correlation coefficient (ECC) is an important parameter while analysing the diversity performance characteristics of a MIMO antenna system. This system has reportedly achieved an ultra-low ECC of 5×10^{-6} making this system appropriate to MIMO applications in this frequency band. FSS is an attractive candidate for mitigation of mutual coupling because of the flexibility it provides as far as the operating band is concerned. Yet another system operating in the frequency band of 30GHz employing crossed-dipole structures on the FSS has been reported¹⁴ and it is very clear from the results of the investigations, varying degrees of isolation enhancement are achievable through optimization of the FSS for operation in a frequency band of interest. The air gap technique¹⁹ is implemented in aperture coupled antenna design to improve the gain.

Recently surface wave attenuation in a patch array antenna was accomplished using a capacitively loaded loop metamaterial (CLL-MTM) superstrate and more than 55dB isolation was achieved at a centre frequency of 3.3GHz. This CLL-MTM will be very much useful in LTE communication systems as it can be used to improve the isolation of array antennas already in use, eliminating the necessity of replacing them with new ones¹⁵. A self-diplexing MIMO antenna improving the isolation has been reported^{20,21}. In this paper a dual element antenna system is proposed for MIMO applications in the frequency band of 7.525-9.1GHz. To reduce the mutual coupling an MTM array is inserted in between two CSRR radiating elements. The radiating elements are stimulated through aperture coupling technique to increase the gain.

2 | Antenna Design

The proposed MIMO antenna design involves five stages from antenna A to antenna E. Single circular patch antenna A and MTM loaded antenna B are presented in Fig. 1. Though there exists a variety of options to load the MTM structure, aperture coupled MTM antenna loaded with air gap between two substrates is implemented to achieve high gain with bandwidth

enhancement. The first stage of the antenna is designed with a single circular patch. In the second stage, the famous circular NBCSRR printed as a radiating element on the upper surface of the substrate. In both cases, FR4-epoxy with a dielectric constant ϵ_r of 4.4 with a dielectric loss $\tan\delta = 0.002$ is used. The aperture is made in the ground layer on the top of the bottom substrate and the feed line is provided in the bottom surface of the lower substrate of antenna B and the radiating element is printed on the top surface of the upper substrate as depicted in Fig. 2.

2.1 | Schematic of aperture coupling

Depicted in Figure.3 is a comprehensive picture of the aperture coupling realized in the present design of an all MTM MIMO. The feedline is printed on the bottom surface of the lower substrate. Meanwhile the ground plane is printed on the top surface of this substrate. Carved out of the same is an aperture of dimension 8mm x 1.3mm directly below the radiating element of each antenna. The radiating elements of the antennas are printed on the upper surface of the other substrate viz. the top substrate

2.2 | The proposed Design

The optimized values of the geometrical dimensions of the antenna are given in Table 1. The overall size of the antenna is 30mm x 16mm x 4.7mm. The antenna is excited through the bottom edge of the microstrip line and is powered up through an SMA connector. As shown in Fig. 4, in antenna C and D an additional antenna element is printed to realize the MIMO antenna design.

Table 1
Dimensions of the proposed antenna

Parameter	Dimension (mm)	Parameter	Dimension (mm)
L	16	S_w	1.3
W	16	S	4
L_s	10	r_1	4.9
W_s	2	r_2	4
S_1	8	r_3	2.5
L_a	16	g	0.8
W_a	30	S_1	0.8
D	8.9	d	4
W_a	30	h	1.5

Two NBCSRR elements of outer ring radii $r_1 = 4.9$ mm with a distance of separation of the order of $\lambda_0/8.3$ (4mm) are printed on the superstrate of FR4 -epoxy with lateral dimensions $L_a = 16$ mm, $W_a = 30$ mm and thickness 1.6mm. The dimensions of the substrate containing ground, aperture ($S_w \times S_1 = 1.3$ mm x 8mm) and the microstrip feedlines ($W_s = 2$ mm) are also the same.

An air gap of around 1.5mm has been maintained between the superstrate and the substrate to achieve a gain of 8.15dB at the resonant frequency of 8.5GHz.

Though the MTM radiating elements loaded in antenna D are self diplexing, mutual coupling is greatly reduced only after inserting the rectangular vertical MTM array in between the two radiating elements as shown in Fig. 5 and all the

characteristics of the antenna are simulated through finite element based HFSS, an Ansys software.

3 | Parametric Analysis

The primary goal of the present antenna design is isolation between the radiating elements. Keeping this in mind, the air gap h , the stub length S and the aperture length S_1 are given importance in this analysis.

3.1 | Air gap optimization

Figure 6 shows that the resonant frequency shifted in the direction of positive x values as the air gap height h value increases from zero. At the value of 1.5mm of h , the antenna achieves a gain of 8.15dB as depicted in Fig. 12(a) with a bandwidth of about 1.575GHz. This prompted us to decide upon the optimized value of $h = 1.5$ mm.

3.2 | Stub length S optimization.

The stub length is one of the main components to effect improvement in the return loss. Stub length S improves the return loss about -40dB in its 4mm value at the resonant frequency of 8.5GHz while effecting insignificant variation in its other values, viz. 3mm, 3.5mm, 4.5mm and 5mm, as depicted in Fig. 7. Hence the optimized stub length value has been taken as $S = 4$ mm.

3.3 | Aperture length S_1 optimization

Aperture length S_1 is one of the major elements in this type of antenna to stimulate the radiating element. The aperture length is properly chosen to resonate the antenna over the desired band of frequency. Hence, the aperture length S_1 is optimized at the value of 8mm in the resonant frequency of 8.5GHz with a return loss of -40dB which has been delineated in Fig. 8.

3.4 | Antenna fabrication

After the optimization of the parameters, an antenna prototype has been fabricated which is shown in Fig. 9.

4 | Results And Discussion

To ascertain the impact of the non-bianisotropic nature of the MTM unit cell on bandwidth enhancement, return loss simulation was carried out on the fabricated prototype loaded with a simple CSRR also and the results are presented in Fig. 10. The proposed MIMO antenna is resonating at 8.5GHz (useful in X band wireless applications). It is to be noted that unlike the many MTM antennas reported in the literature, the proposed antenna exceptionally achieves a wide fractional -10dB impedance bandwidth of 18.94% in the frequency range of 7.525GHz - 9.1GHz.

The measured and simulated S-parameters of the antennas are presented in Fig. 11. ENA series E5071C Vector Network Analyser (VNA) was employed in the S-parameter measurements on the prototype. Good agreement between the measured and simulated values is distinctive from the curves. The slight discrepancy in the return loss curves could be due to the fabrication tolerance and the parasitic arising out of the soldering. From the curves, it is concluded that the isolation is maintained up to 47dB in between the measured values of S_{11} and S_{21} in the operating frequency band.

Figure 12 (a) shows that the gain is gradually increasing when the air gap value increases from zero to 1.5mm. At zero-air gap, a gain of 3dB is maintained through the bandwidth. It has been increased up to 8.15dB when the air gap is kept at 1.5mm. It has to be noted that air gap variation is possible only if the antenna is designed with aperture coupling.

Additionally, efficiency of the antenna is also increased from 50–81.14% when the air gap is varied from 0 to 1.5mm. Iteration of antenna gain and efficiency are depicted in Fig. 12 (a) and 12(b).

4.1 | Radiation Patterns

Simulated and measured radiation patterns of the proposed antenna for the targeted frequency is given in Fig. 13. It is clear from these radiation patterns that the proposed antenna radiates in dipolar fashion in the xy-plane and thus the E plane radiation pattern is bidirectional and the H plane (xz plane) radiation pattern is omnidirectional.

The simulated and measured results of the transmission coefficients are presented in Fig. 14. It is clear from the profiles that the antennas C to E achieve an isolation of up to 47dB in the operating frequency band. Besides, it is clear that the measured S_{21} values of antenna E does curve similar to the simulated values. From the curves, it is obvious that MTM loaded antenna D has self-diplexing capacity.

Isolation is an important parameter of MIMO antenna which can be measured from envelope correlation coefficient (ECC) value. It is an indicator of interaction of element antennas of MIMO. Having a small ECC value is very important to approve the usefulness of the proposed antenna. ECC is computed using the following formula¹³ 1.

$$\rho_e = \frac{|S_{11}^* S_{12} + S_{21}^* S_{22}|^2}{(1 - |S_{11}|^2 - |S_{21}|^2)(1 - |S_{22}|^2 - |S_{12}|^2)} \quad (1)$$

From Fig. 15, the fabricated prototype maintains an ECC of 0.015 over the resonant frequency of 8.5GHz. The ECC value over the targeted frequency band is less than 0.025. Performance comparison with previous works are given in Table 2.

Table 2
Comparison of performance with previous works

Ref.	No. of elements	Radiating element	Isolating structure	Edge to edge spacing (mm)	Isolation (dB)	Gain (dB)	Efficiency (%)	ECC
Hafezifard ²	2	Meander Line	Metamaterial	5	19	5.7	77.6	Not specified
Marina ³	2	Patch	EBG	15	20	Not specified	85.9	Not specified
Dadgarpour ⁴	2	DRA	Metamaterial	2.5	46.5	7.90	91	Not specified
Qian ⁹	2	Patch	EBG	1	20	Not specified	83	Not specified
Jian ¹⁸	2	Patch	Not given	5	15	4.2	60	.02
This work	2	Metamaterial	Metamaterial	4	47	8.15	84.14	0.015

5 | Conclusion

An all MTM MIMO antenna has been designed and implemented to improve isolation between two NBCSRR elements. An MTM array placed in between the two MTM radiating elements plays a major roll to suppress the mutual coupling. Measured values show that an isolation of nearly 47dB is achieved with the decoupling technique in the operating frequency band of 7.525GHz to 9.1GHz. This antenna is most suitable for military applications.

Declarations

Funding: Not Applicable

Availability of data and materials: Not applicable.

Compliance with Ethical Standards

Conflict of interest The authors declare that they have no competing interests.

Code availability: Not Applicable

References

1. Xiaoming Chen, Shuai Zhang, Qinlong Li. A review of mutual coupling in MIMO systems, *IEEE Access*. 2018;6:24706-24719.
2. Hafezifard R, Naser-Moghadasi M, Rashed Moassel J, sadeghzadeh R A. Mutual coupling reduction for two closely spaced meander line antennas using metamaterial substrate. *IEEE Antennas Wirel Propag Lett*. 2016; 15:40-43.
3. Marina Mavridou, Alexandros P.Feresidis, Peter Gardner. Tunable Double-Layer EBG structures and application to antenna isolation. *IEEE Trans Antennas Propag*. 2016; 64(1):70-79.
4. Dadgarpour A, Bal S. Virdee, Tayeb A. Denidni, A. Kishk. Mutual coupling reduction in dielectric resonator antennas using metasurface shield for 60-GHz MIMO systems. *IEEE Antennas Wirel Propag Lett*. 2017; 16:477-479.
5. Ramasamy Pandeewari, Singaravelu Raghavan. Broadband monopole antenna with split ring resonator loaded substrate for good impedance matching. *Microw Opt Techn Lett*. 2014; 56(10):2388-2392.
6. Pandeewari R, Raghavan S. Microstrip antenna with complementary split ring resonator loaded ground plane for gain enhancement. *Microw Opt Techn Lett*. 2015; 57(2):292-296.
7. Pandeewari R, Raghavan S. Meandered CPW -fed hexagonal split-ring resonator monopole antenna for 5.8 Ghz RF-ID applications. *Microw Opt Techn Lett*. 2015; 57(3):681-684.
8. Pandeewari R, Raghavan S. A CPW-fed triple band OCSRR embedded monopole antenna with modified ground for WLAN and WIMAX applications. *Microw Opt Techn Lett*. 2015; 57(10):2413-2418.
9. Qian Li, Alexandros P. feresidis, Marina Mavridou, Peter S.Hall. Miniaturized double-layer EPG structures for broadband mutual coupling reduction between UWB monopoles. *IEEE Trans Antennas Propag.*, 2015; 63(3): 1168-1171.
10. Guohua Zhai, Zhi Ning Chen, Xianming Qing. Enhanced isolation of a closely spaced four-element MIMO antenna system using metamaterial mushroom. *IEEE Trans Antennas Propag*. 2015; 63(8): 3362-3370.
11. K-L. Wu, C. Wei, X. Mei, Z. -Y. Zhang. Array-antenna decoupling surface. *IEEE Trans Antennas Propag*. 2015;5(12):6728-6738.
12. Mei Jiang, Zhi Ning Chen, Yan Zhang, Wei Hong, Xiaobo Xuan. Metamaterial-based thin planar lens antenna for spatial beamforming and multibeam massive MIMO. *IEEE Trans Antennas Propag*. 2017;65(2):464-472.
13. Reza Karimian, Arun Kesavan, Mourad Nedil Tayeb, A Denidni. Low-mutual-coupling 60-GHz MIMO antenna system with frequency selective surface wall. *IEEE Antennas and wirel propag lett*. 2017;16:373-376.
14. Mohammad Akbari, Hamdan Abo Chalyon, Mohammadmahdi Farahani, Abdel-Razik Sebak, Tayeb A Denidni. Spatially decoupling of CP antennas based on FSS for 30-GHz MIMO systems, *IEEE Access*, 2017;5:6527-6537.
15. Ali Jafargholi, Amir Jafargholi, Jun H. Choi. Mutual coupling reduction in an array of patch antennas using CLL metamaterial superstrate for MIMO applications. *IEEE Trans Antennas Propag*. 2019;67(1):179-189.
16. Yun Hu, Wei Hong, Zhi Hao Jiang. A multibeam folded reflectarray antenna with wide coverage and integrated primary sources for millimeter-wave massive MIMO applications. *IEEE Trans Antennas Propag*. 2018;66(12):6875-6882

17. Kunal Srivastava, Ashwani Kumar, Binod K.Kanaujia, Santanu Dwari, Sachin Kumar. A CPW-fed UWB MIMO antenna with integrated GSM band and dual band notches. *Int J RF and Microw comp-Aided Eng.* 2019;29:e21433.
18. Jian Ren, Wei Hu, Yingzeng Yin, Rong Fan. Compact printed MIMO antenna for UWB applications. *IEEE Antennas Wirel Propag Lett.* 2014;14:1517-1520.
19. Nornikman Hassan, Zahriladha Zkaria, Weng Yik Sam, Izyan Nazihan Mohd Hanapiah, Nasoruddin Mohamad A, Ameer Farhan Roslan, Badrul hisham Ahmad, Mohd Khairy Ismail, Mohamad Zoinol Abidin Abd Aziz. Design of dual -band microstrip patch antenna with right-angle triangular aperture slot for energy transfer application. *Int J RF and Microw comp-Aided Eng.* 2019;29:e21666.
20. Anping Zhao, Zhouyou Ren. Multiple-input and multiple-output antenna system with self-isolated antenna element for fifth-generation mobile terminals. *Microw Opt Techn Let.* 2019; 61:20-27.
21. Sourav Nandi, Akhilesh Mohan. A self-diplexing MIMO antenna for WLAN applications. *Microw Opt Technol Let.* 2019; 61:239-244.

Figures

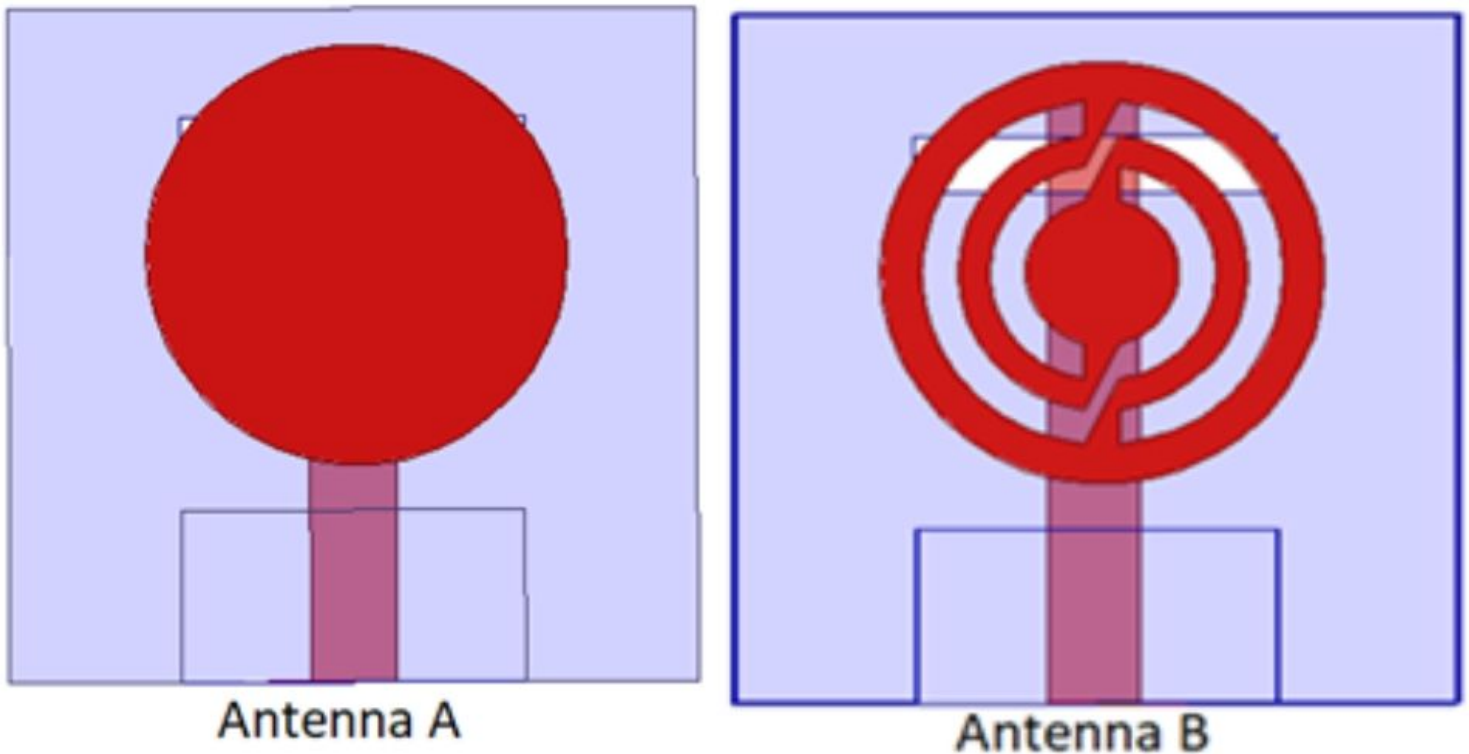


Figure 1

Circular patch antenna A and MTM loaded antenna B

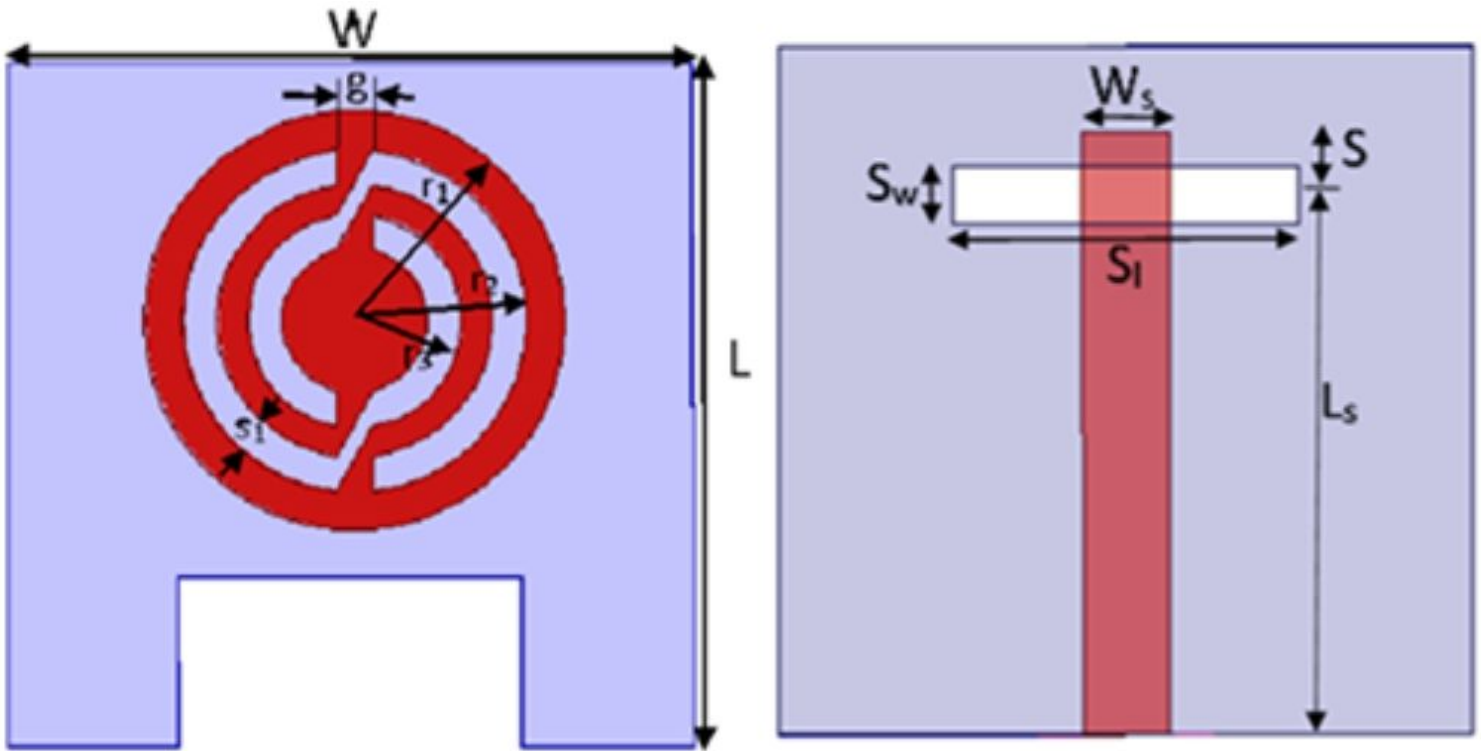


Figure 2

Geometry of the antenna top view, bottom with slotted ground

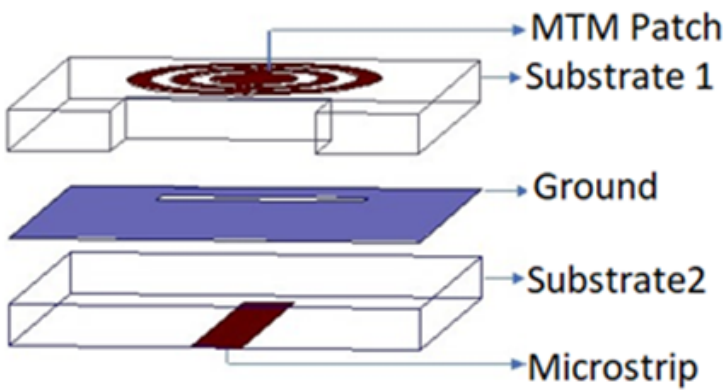


Figure 3

Aperture coupling with two substrates with single MTM element

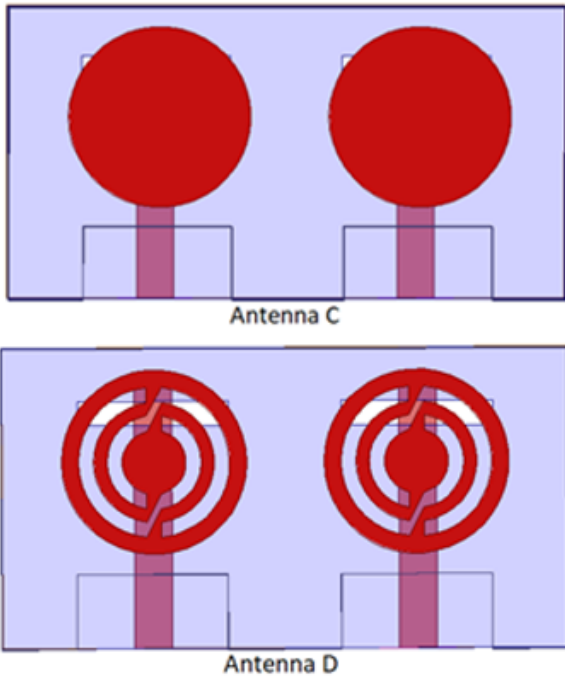


Figure 4

Two patch Antenna C and 2MTM element antenna D

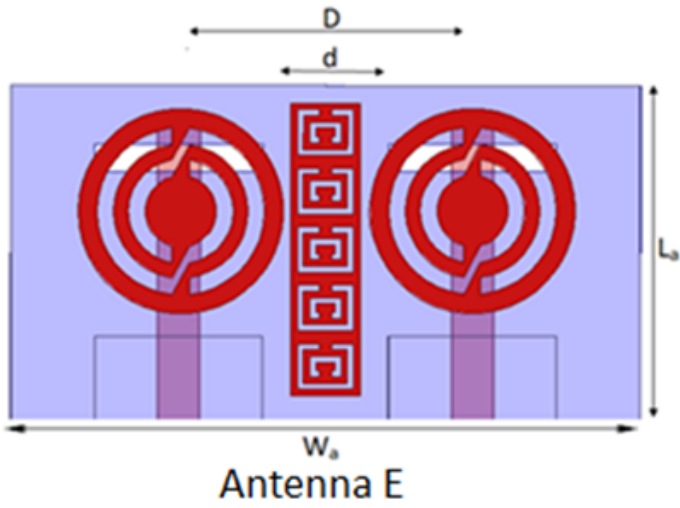


Figure 5

proposed antenna with two MTM element with centre CSRR array

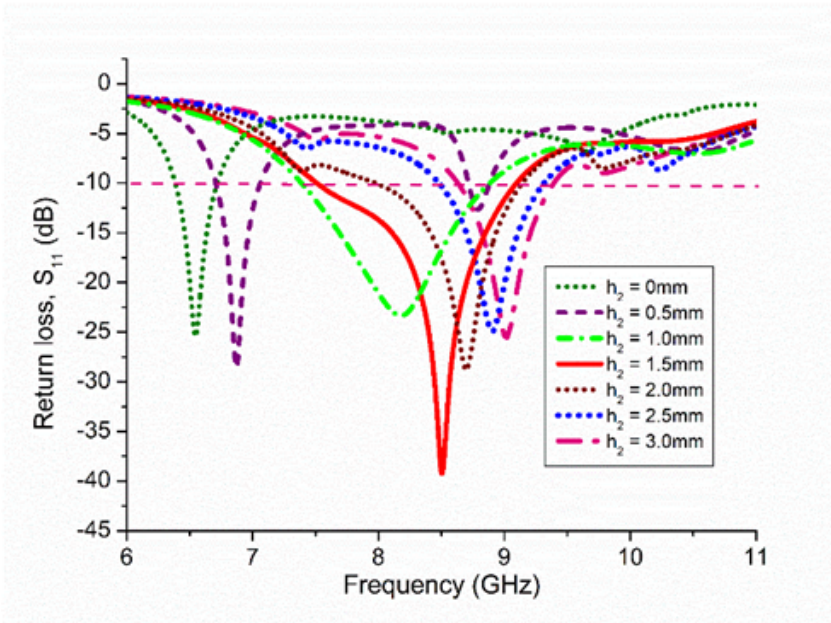


Figure 6

Simulated return loss variation with frequency for various values of h (air gap height)

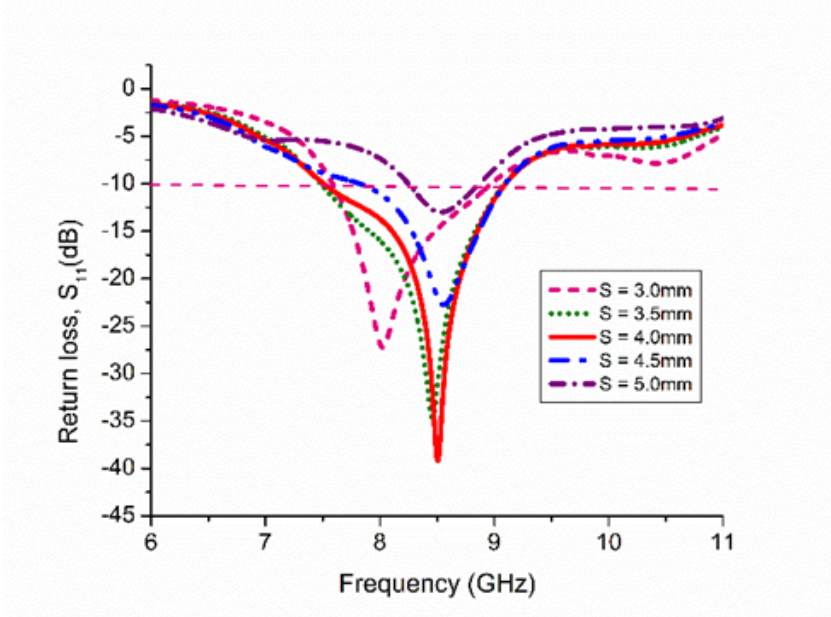


Figure 7

Simulated return loss variation with frequency for various values of S

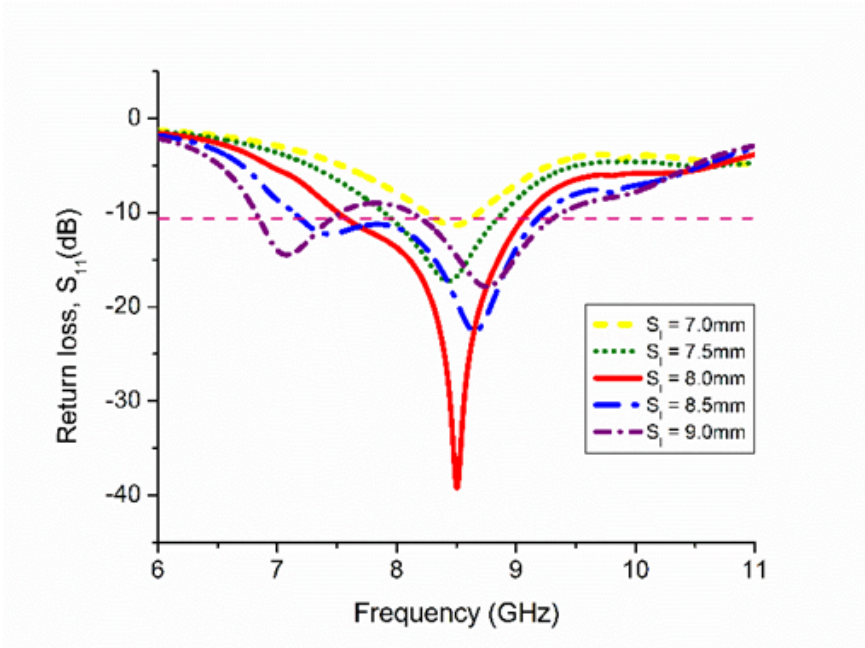


Figure 8

Simulated return loss variation with frequency for various values of SI

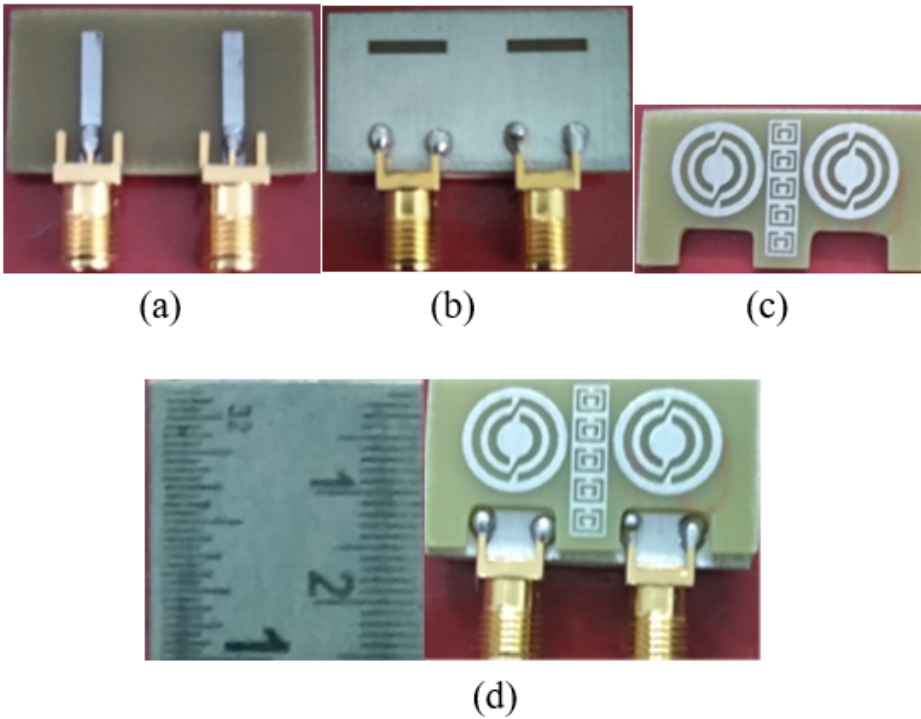


Figure 9

(a) Bottom of the substrate, (b) Top of the substrate, (c) Top of the superstrate and (d) Top view of the fabricated prototype

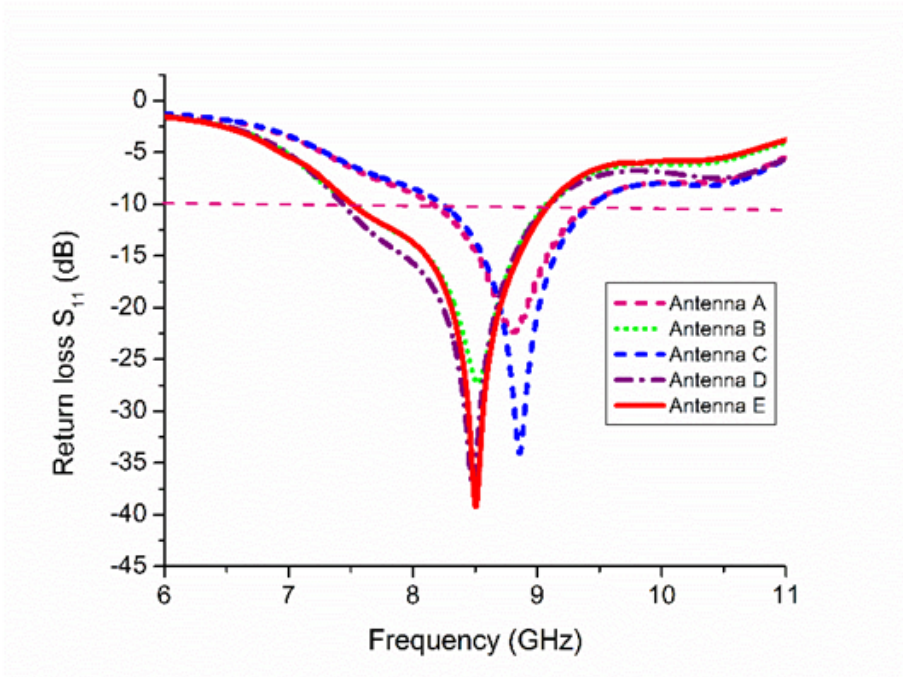


Figure 10

Simulated return loss variation with frequency for the antennas A to E

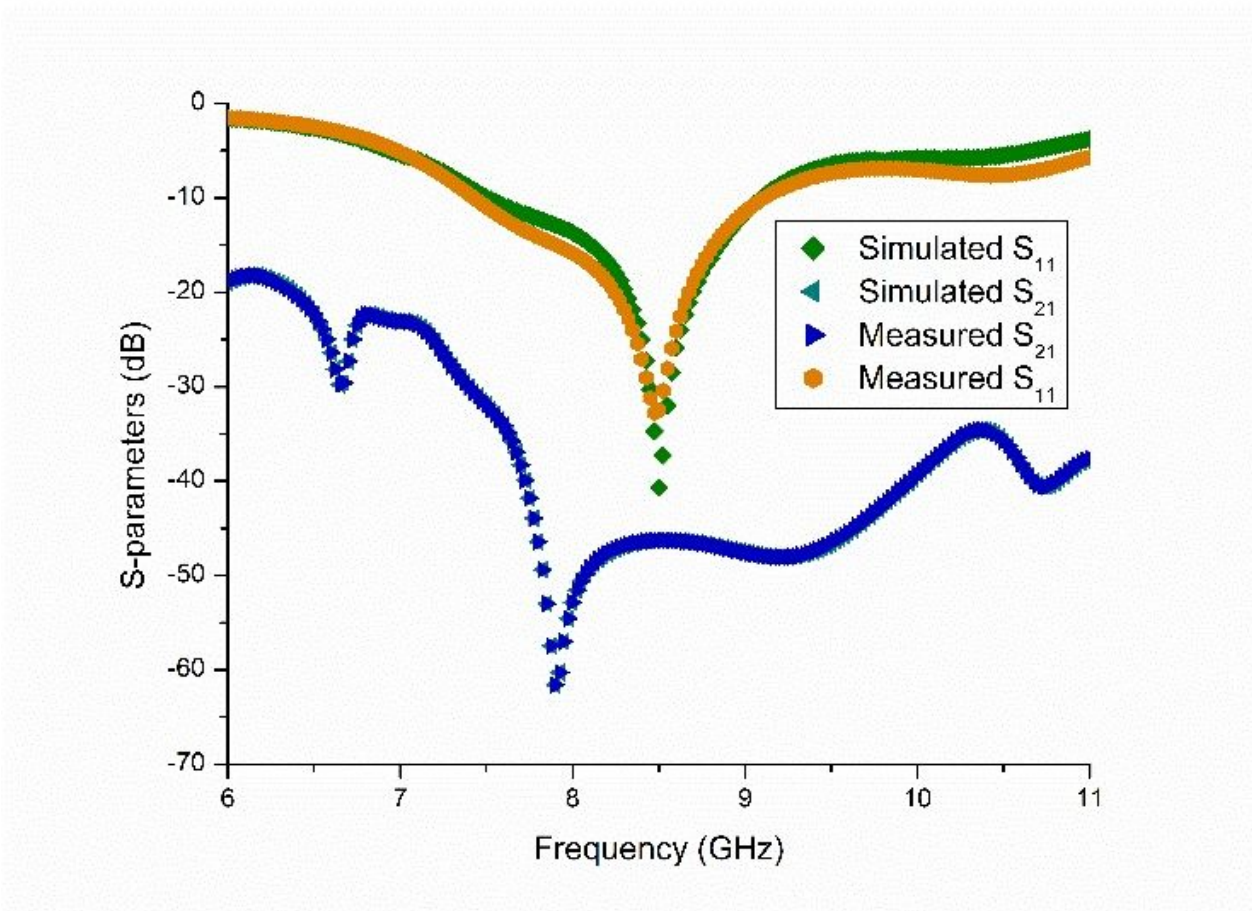


Figure 11

Simulated and measured S-parameters of the antenna

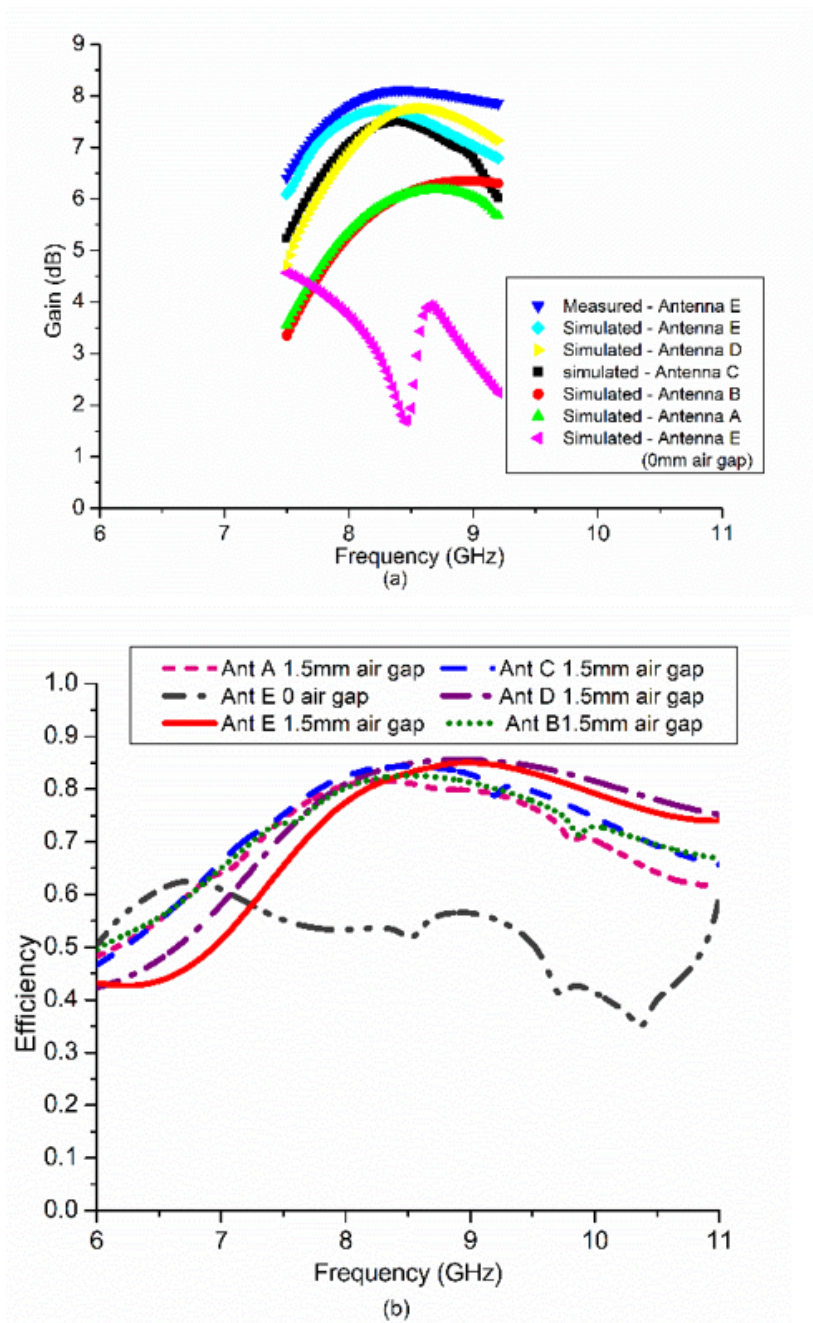


Figure 12

(a) simulated and measured value of the antenna Gain and (b) Efficiency of the antenna A to E in the air gap of 1.5mm and 0 mm

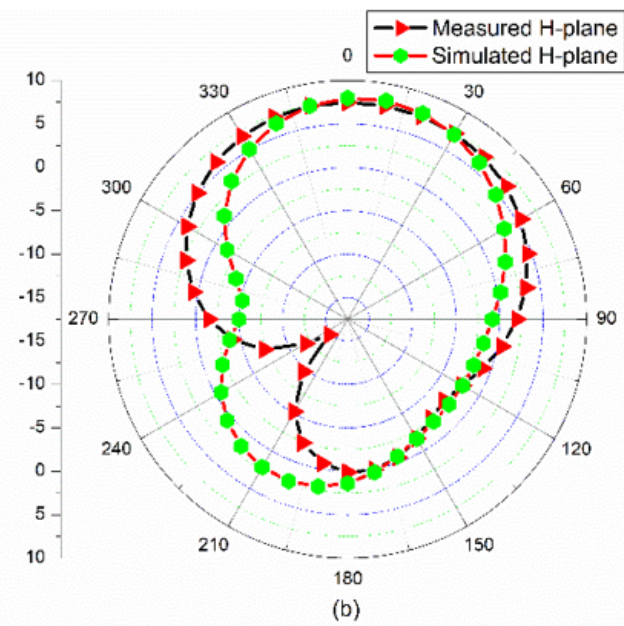
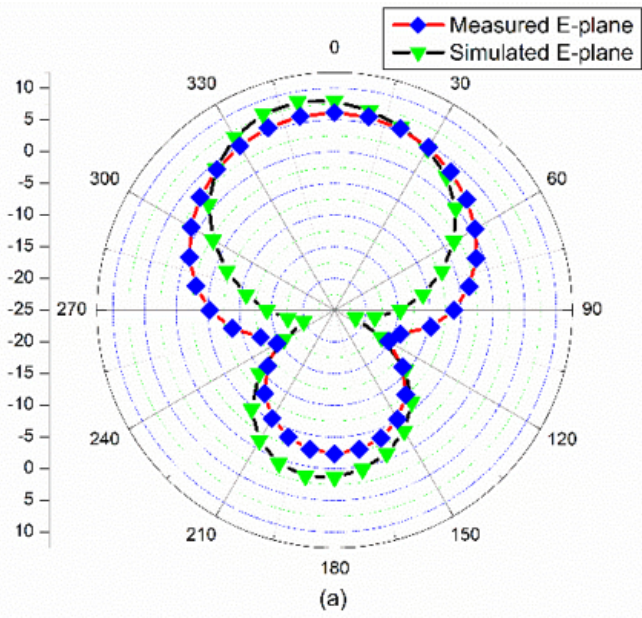


Figure 13

Simulated and measured radiation patterns of the antenna (a) E-Plane and (b) H- Plane

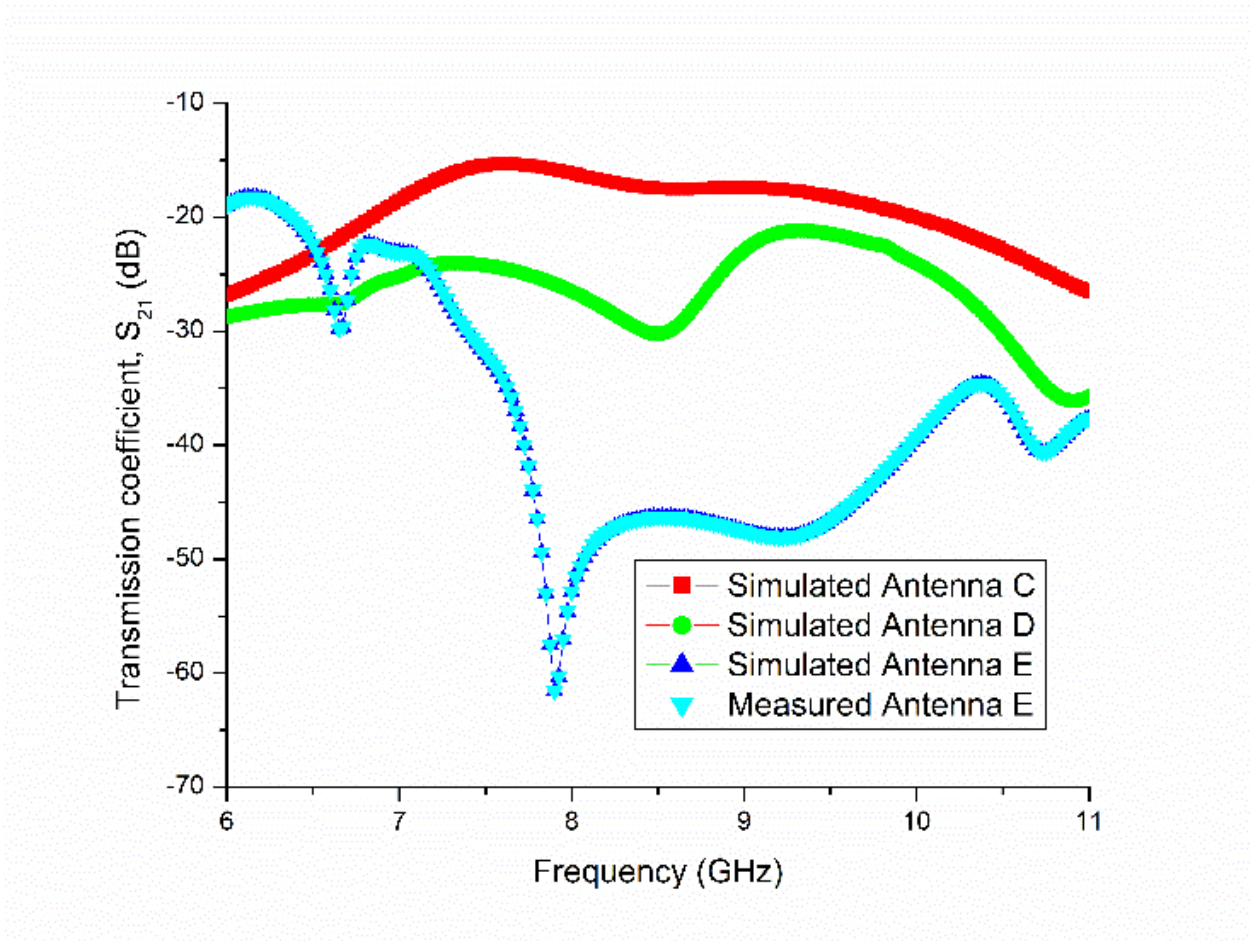


Figure 14

Comparison of Transmission coefficients for antennas C to E with the measured values

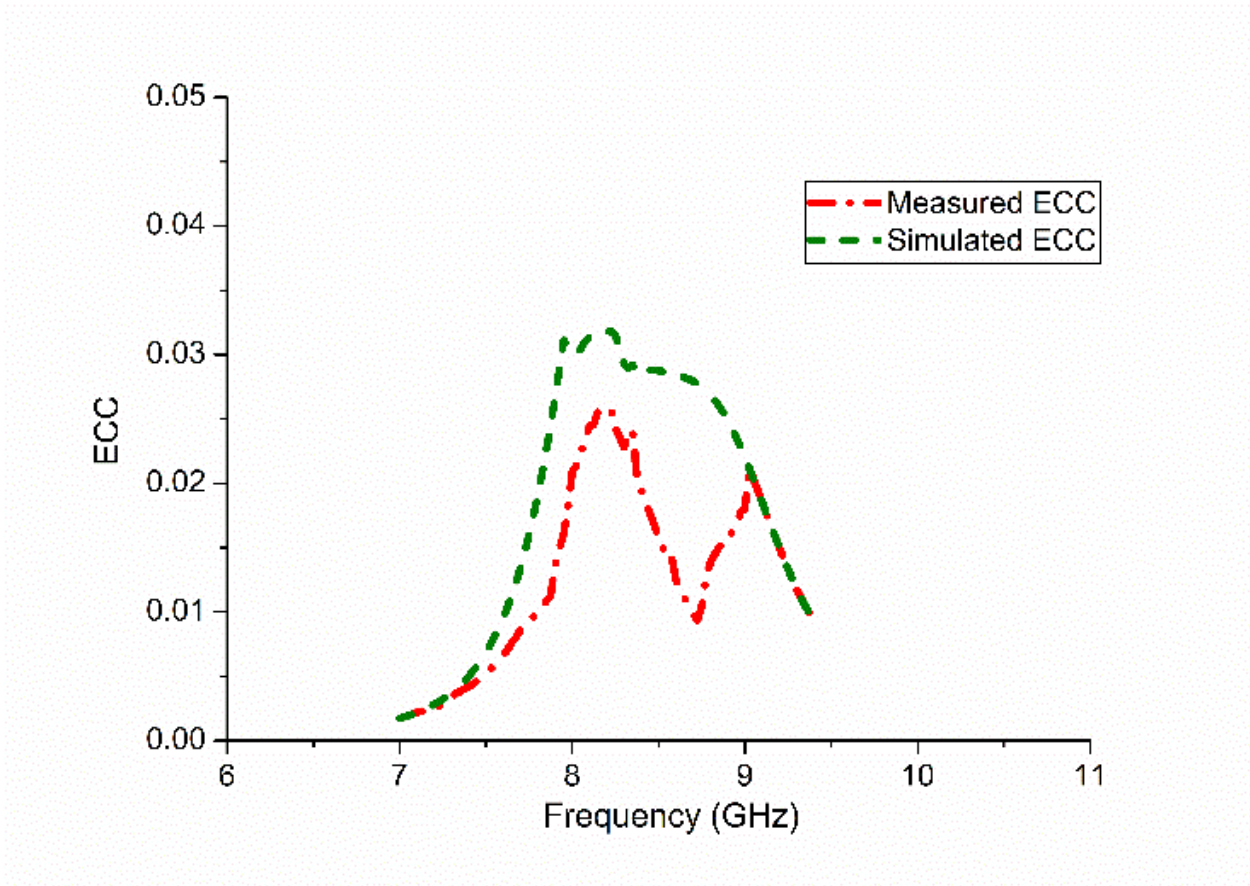


Figure 15

Simulated and Measured value of ECC